

LETTER TO THE EDITOR

Supernova 2008J: early time observations of a heavily reddened SN 2002ic-like transient*

F. Taddia¹, M. D. Stritzinger², M. M. Phillips³, C. R. Burns⁴, E. Heinrich-Josties⁴, N. Morrell³, J. Sollerman¹, S. Valenti⁵, J. P. Anderson⁶, L. Boldt⁷, A. Campillay³, S. Castellon³, C. Contreras³, G. Folatelli⁸, W. L. Freedman⁴, M. Hamuy⁶, W. Krzeminski⁹, G. Leloudas^{10,11}, K. Maeda⁸, S. E. Persson⁴, M. Roth³, and N. B. Suntzeff^{12,13}¹ The Oskar Klein Centre, Department of Astronomy, Stockholm University, AlbaNova, 10691 Stockholm, Sweden² Department of Physics and Astronomy, Aarhus University, Ny Munkegade 120, DK-8000 Aarhus C, Denmark³ Carnegie Observatories, Las Campanas Observatory, Casilla 601, La Serena, Chile⁴ Observatories of the Carnegie Institution for Science, 813 Santa Barbara Street, Pasadena, CA, USA⁵ INAF-Osservatorio Astronomico di Padova, vicolo dell'Osservatorio 5, 35122 Padova, Italy⁶ Departamento de Astronomia, Universidad de Chile, Casilla 36D, Santiago, Chile⁷ Argelander Institut für Astronomie, Universität Bonn, Auf dem Hügel 71, D-53111 Bonn, Germany⁸ Kavli Institute for the Physics and Mathematics of the Universe (IPMU), University of Tokyo, 5-1-5 Kashiwanoha, Kashiwa, Chiba 277-8583, Japan⁹ N. Copernicus Astronomical Center, ul. Bartycka 18, 00-716 Warszawa, Poland¹⁰ The Oskar Klein Centre, Department of Physics, Stockholm University, AlbaNova, 10691 Stockholm, Sweden¹¹ Dark Cosmology Centre, Niels Bohr Institute, University of Copenhagen, 2100 Copenhagen, Denmark¹² Department of Physics and Astronomy, Texas A&M University, College Station, TX 77845, USA¹³ The Mitchell Institute for Fundamental Physics and Astronomy, Texas A&M University, College Station, TX 77845, USA

Received 26 July 2012 / Accepted 21 August 2012

Abstract

Aims. We provide additional observational evidence that some Type Ia supernovae (SNe Ia) show signatures of circumstellar interaction (CSI) with hydrogen-rich material.

Methods. Early phase optical and near-infrared (NIR) light curves and spectroscopy of SN 2008J obtained by the *Carnegie Supernova Project* are studied and compared to those of SNe 2002ic and 2005gj. Our NIR spectrum is the first obtained for a 2002ic-like object extending up to $2.2 \mu\text{m}$. A published high-resolution spectrum is used to provide insight on the circumstellar material (CSM).

Results. SN 2008J is found to be affected by $A_V \sim 1.9$ mag of extinction and to closely resemble SN 2002ic. Spectral and color comparison to SNe 2002ic and 2005gj suggests $R_V < 3.1$. Spectral decomposition reveals the underlying SN emission matches a 1991T-like event and, since SN 2008J is as luminous as SN 2005gj ($V_{\text{max}} = -20.3$ mag), we conclude that their CSI emissions are similarly robust. The high-resolution spectrum reveals narrow emission lines produced from un-shocked gas characterized by a wind velocity of $\sim 50 \text{ km s}^{-1}$. We conclude that SN 2008J best matches an explosion of a SN Ia that interacts with its CSM.

Key words. supernovae: general – supernovae: individual: SN 2008J

1. Introduction

Supernova (SN) 2002ic was the first event identified as a Type Ia SN interacting with hydrogen-rich circumstellar material (CSM) (Hamuy et al. 2003; Wood-Vasey et al. 2004). Spectroscopically similar to the bright SN 1991T, the spectral energy distribution of SN 2002ic also exhibited prevalent narrow Balmer emission lines which are typically produced by SN–CSM interaction (CSI) in Type II core-collapse (CC) SNe. In SN 2002ic, the CSI explains not only its high peak bolometric luminosity ($L_{\text{bol}} \approx 3 \times 10^{43} \text{ erg s}^{-1}$) and slow declining light curve, but also its strong, broad hydrogen, calcium, and iron features observed at late epochs (Chugai et al. 2004). SN 2002ic-like events are extremely rare. To date only SN 1997cy (Germany et al. 2000; Turatto et al. 2000; Hamuy et al. 2003; Deng et al. 2004), SN 1999E (Rigon et al. 2003), SN 2005gj (Aldering et al. 2006;

Prieto et al. 2007) and PTF11kx (Dilday et al. 2012) have been found to resemble SN 2002ic. Given the rarity of this kind of transient, and the opportunity they offer to better understand the progenitors of SNe Ia, it is imperative to enlarge the observational sample of 2002ic-like SNe. This letter presents early-time optical and near-infrared (NIR) observations of the 2002ic-like SN 2008J obtained by the *Carnegie Supernova Project* (CSP; Hamuy et al. 2006).

2. Observations

SN 2008J was discovered near the center of the SBbc galaxy MGC–02–07–033 on 15.2 January 2006 UT (Thrasher et al. 2008), and two days later was classified as a Type-Ia/II SN (Stritzinger et al. 2008). According to Theureau et al. (1998) (via NED), the redshift of the host is $z = 0.0159$, which corresponds to a luminosity distance of 66.3 ± 1.2 Mpc, when we adopt WMAP5 cosmology and corrections for peculiar motions. The CSP began photometric follow-up 4 days after discovery

* Based on observations collected at the European Organisation for Astronomical Research in the Southern Hemisphere, Chile (ESO Programme 080.A–0516).

and continued over the course of 34 days. In doing so, 10 epochs of optical and 6 epochs of NIR imaging were obtained with the 1-m Swope telescope at Las Campanas Observatory. All science images were reduced in a standard manner following methods described in Contreras et al. (2010). Photometry of the SN was computed differentially with respect to local sequence stars. Optical and NIR local sequences in the standard photometric systems are listed in Table 1, and optical and NIR photometry in the *natural system* of the Swope telescope is presented in Tables 2 and 3. Fig. 1 displays the absolute magnitude optical and NIR light curves of SN 2008J, compared to those of SNe 2002ic and 2005gj. The CSP obtained three optical spectra of SN 2008J, which were reduced following the method described by Hamuy et al. (2006). A high-resolution optical spectrum was acquired by Sternberg et al. (2011). This spectrum is used to place constraints on the nature of the CSM. A NIR spectrum of SN 2008J was also obtained with the NTT 5 days before B -band maximum (B_{\max}). This is the first published NIR spectrum of a 2002ic-like object extending up to $2.2 \mu\text{m}$. A log of these spectral observations is given in Table 4 and the data are plotted in Figs. 2–4.

3. Results

The spectral sequence reveals prevalent Na I D absorption and a diffuse interstellar band (DIB, $\lambda 6284$) at the SN rest frame (see Fig. 2, left panel inset), which are indicative of significant host dust extinction (Galactic extinction is only $A_V = 0.062$ mag, Schlafly & Finkbeiner 2011, via NED). Significant reddening is also consistent with the heavily suppressed blue-end of the optical spectrum, and with the mid-IR dust emission documented by Fox et al. (2011). We turn to the high-resolution spectrum shown in Fig. 4 (top-left panel), in order to fit Gaussians to the individual Na I D components. We obtain total equivalent widths (EWs) of Na I D₂ = 1.87 \AA and Na I D₁ = 1.47 \AA . These measurements indicate that the absorption features are saturated and that $E(B - V)_{\text{host}}$ exceeds 0.5 mag (Turatto et al. 2003, although see Poznanski et al. 2011) for $R_V = 3.1$ (Cardelli et al. 1989).

The first optical and the NIR spectra are used to estimate an upper limit on $E(B - V)_{\text{tot}}$, through the Balmer decrement and the comparison of $P\beta$ to $H\alpha$ and $H\beta$ ratios to theoretical expectations. This limit is R_V -dependent and we note that several studies (e.g. Wang et al. 2008; Folatelli et al. 2010) revealed that R_V values for SNe Ia may differ from that of normal interstellar dust, pointing to R_V as low as 1.5. We find $E(B - V)_{\text{tot}} \leq 0.8 \pm 0.2$ mag and 1.3 ± 0.3 mag for $R_V = 3.1$ and 1.5 respectively.

In Fig. 1 we compare the absolute magnitude light curves of SN 2008J, corrected for these two different reddenings, with those of SNe 2002ic and 2005gj. Peak apparent and absolute magnitudes of SN 2008J are listed in Table 6. SN 2008J peaked first in the u - and B -bands, and subsequently at longer wavelengths. For $R_V = 1.5$ coupled with $E(B - V)_{\text{tot}} = 1.3$ mag, SN 2008J appears to be as luminous as SN 2005gj in each of the passbands. Instead, for a $R_V = 3.1$ and $E(B - V)_{\text{tot}} = 0.8$ mag, peak magnitudes would be significantly brighter (0.5–0.7 mag) in the Vri -bands whereas the u -band peak would be fainter (0.4 mag). Therefore, using the standard $R_V = 3.1$ would make SN 2008J much redder than the other SNe, even for the upper limit $E(B - V)_{\text{tot}} = 0.8$ mag. Instead, a lower R_V gives rise to colors similar to those of SNe 2002ic and 2005gj.

This is confirmed in Fig. 2 (right panel), where the last (de-reddened) spectrum of SN 2008J is plotted along with similar phase spectra of SNe 2002ic and 2005gj. The comparison re-

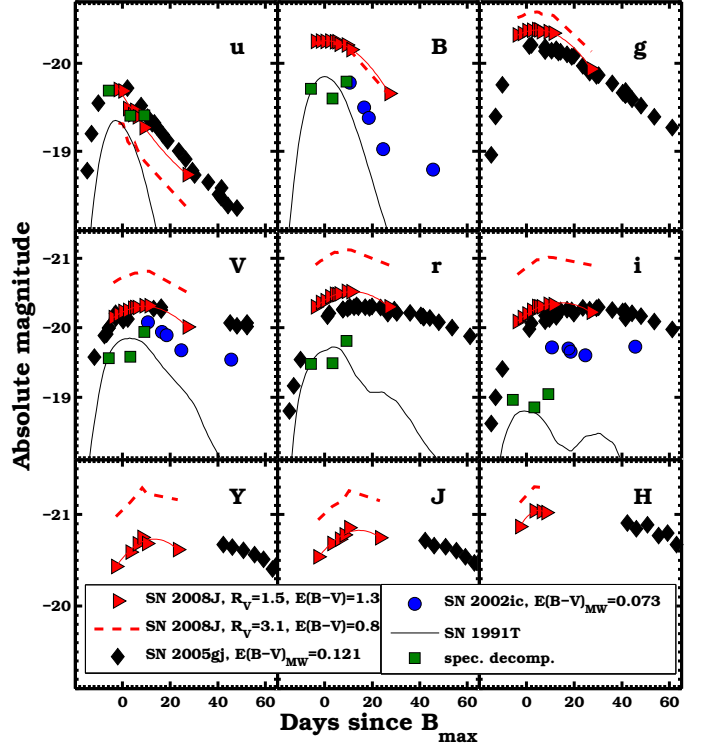


Figure 1: Absolute magnitude light curves of SN 2008J corrected for different amounts of reddening as discussed in the text. For comparison de-reddened absolute magnitudes of SNe 2002ic (Hamuy et al. 2003) and 2005gj (Aldering et al. 2006; Prieto et al. 2007) are also plotted, assuming distance moduli of 37.32 mag and 37.09 mag respectively. Template optical light curves of SN 1991T (Nugent et al. 2002) are plotted and scaled to match the absolute $uBVri$ peak magnitudes of SN 1991T presented by Prieto et al. (2007) and Saha et al. (2001). Synthetic magnitudes from the spectral decomposition of SN 2008J (see also Fig. 3) match reasonably well the SN 1991T templates.

veals that SN 2008J strongly resembles both SNe 2002ic and 2005gj and that its colors are similar to those of the other two SNe for $R_V = 1.5$ and $E(B - V)_{\text{tot}} = 1.3$ mag. Therefore, assuming that 2002ic-like events have similar colors, we adopt $R_V = 1.5$ and $E(B - V)_{\text{tot}} = 1.3^{+0.3}_{-0.2}$ mag. Here the uncertainty of -0.2 mag is obtained from the light curve comparison, which reveals (for the adopted $R_V = 1.5$) that a color excess lower than 1.1 mag would make the u - and B -band peak magnitudes of SN 2008J fainter than those of a 1991T-like event. These assumptions yield a visual extinction of $A_V = 1.93^{+0.45}_{-0.30}$ mag.

The low-resolution optical spectra of SN 2008J are characterized by a red continuum with prevalent $H\alpha$ and $H\beta$ emission lines superposed. The continuum also reveals broad features which become more prominent as the SN is expanding, e.g. the structures with rounded peaks at ~ 4700 , 5600 and 8700 \AA (see Fig. 2, left panel).

After continuum subtraction, the Balmer lines are well represented by the sum of two Lorentzian profiles having the same peak wavelength (see Fig. 4, bottom-left panels). $H\alpha$ and $H\beta$ are characterized by a narrow, unresolved component ($v_n \lesssim 500 \text{ km s}^{-1}$) on top of a broader, resolved component characterized by $v_b \approx 1500 \text{ km s}^{-1}$. Lines having only narrow, unresolved component characterize the first spectrum of

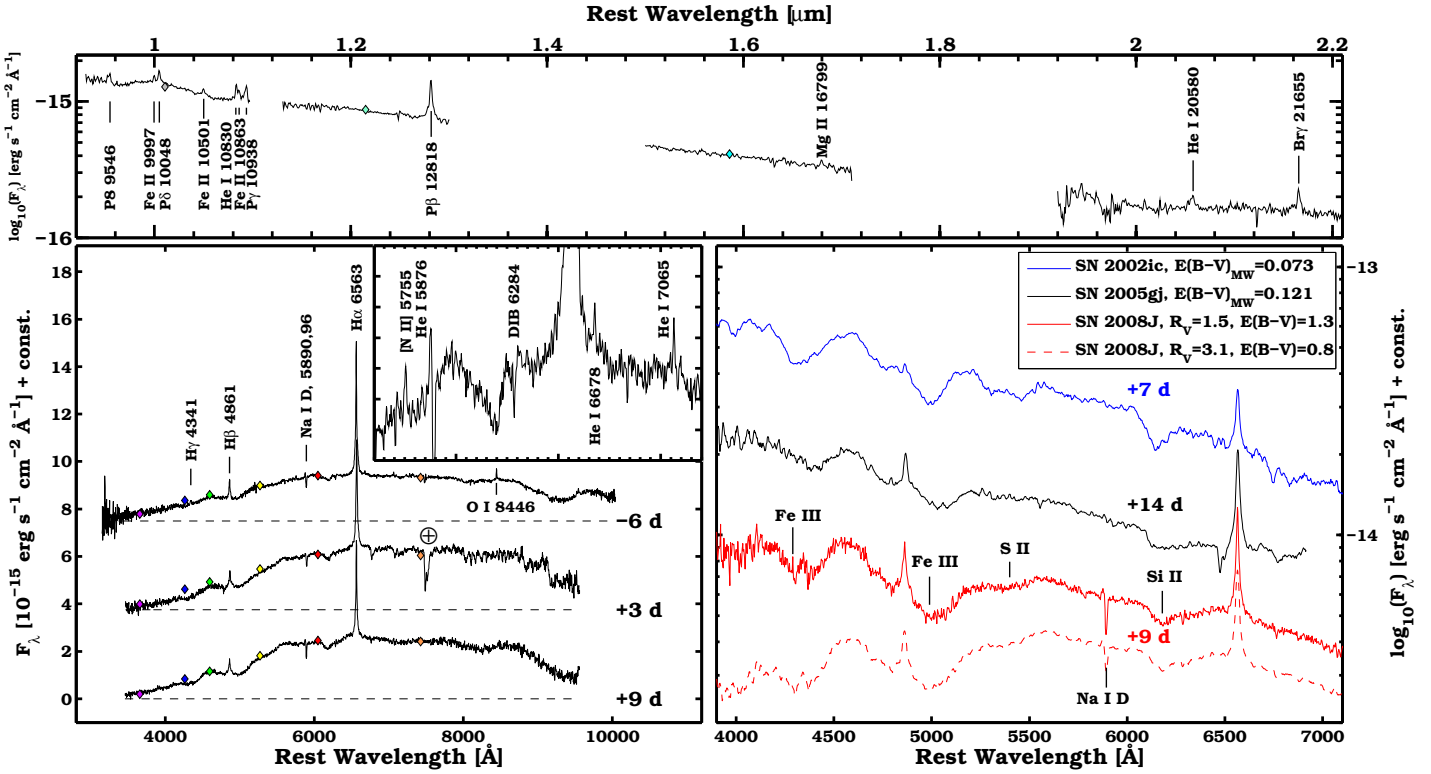


Figure 2: (*Top panel*) NIR spectrum of SN 2008J at 5 days before B_{max} . The spectrum has been scaled to match NIR photometry (colored diamonds). Paschen emission lines as well as He I and Fe II are visible. (*Left panel*) Optical spectroscopy of SN 2008J. Each spectrum has been scaled to match optical photometry. Days since B_{max} are reported, and horizontal dashed lines correspond to zero flux level. Prominent Balmer lines, Na I D, narrow O I $\lambda 8446$ and telluric features are labelled. In the inset we indicate He I narrow emission lines in the first spectrum. Features attributed to [N II] $\lambda 5755$ and diffuse interstellar bands ($\lambda 6284$) are also discernible. (*Right panel*) Spectral comparison of SN 2008J to SNe 2002ic (Hamuy et al. 2003) and 2005gj (Prieto et al. 2007) at comparable epochs. Each spectrum has been de-reddened (see legend).

SN 2008J. In the inset of Fig. 2 we highlight the presence of He I $\lambda\lambda 7065, 6678, 5876$ and N II $\lambda 5755$ features. O I $\lambda 8446$ is also identified in the first spectrum shown in the left panel of Fig 2. Plotted in Fig. 4 (right panels) are 6 narrow lines from the high-resolution ($\sim 5\text{--}8 \text{ km s}^{-1}$) spectrum, 4 of them exhibiting P-Cygni profiles.¹ These features suggest the presence of slowly moving material surrounding the SN, and they exclude the possibility that they are associated with an underlying H II region. Fitting each line with a Lorentzian profile provides a measure of the FWHM, which are summarized in Table 5, and indicates that the CSM has a velocity of $52 \pm 15 \text{ km s}^{-1}$. The high resolution spectrum also exhibits DIBs at $\lambda_0 6284$ and 5780 \AA , having EW = 0.6 \AA and 0.2 \AA respectively.

The broad features in the low-resolution optical spectra are identified through the comparison with SNe 2002ic and 2005gj. The spectra show a dip around $\lambda_0 6180 \text{ \AA}$, which likely originates from Si II $\lambda 6355$ blue-shifted by $\sim 8200 \text{ km s}^{-1}$. Fe III $\lambda 5129$ is probably the line producing the dip at $\sim 4990 \text{ \AA}$, whereas Fe III $\lambda 4404$ absorption is visible at $\sim 4290 \text{ \AA}$. S II $\lambda 5468$ and S II $\lambda 5633$ might cause the depression at $\sim 5400 \text{ \AA}$. The NIR spectrum exhibits narrow, unresolved emission lines, including P β , P δ , P δ , Br γ , He I $\lambda\lambda 10830, 20580$ and Fe II $\lambda\lambda 9997, 10501, 10863$. The bright NIR hydrogen lines (P β , Br γ) are also characterized by a broad component, similar to that observed for the Balmer lines.

4. Discussion

Hamuy et al. (2003) and Aldering et al. (2006) interpreted SNe 2002ic and 2005gj to be SNe Ia interacting with H-rich CSM. This was based mainly on the fact that their spectra are well represented by the sum of two components: a smoothly varying continuum (produced by the CSI) and a diluted spectrum of a 1991T-like SN at comparable phase. In Fig. 3 we show a similar decomposition for the 3 optical spectra of SN 2008J, where we used low-order polynomials to fit the continuum. The models match the spectra reasonably well, especially the Si II dip at $\sim 6200 \text{ \AA}$, and the features between $\sim 3500\text{--}5000 \text{ \AA}$. However, the rounded peak at $\sim 5600 \text{ \AA}$ is not perfectly reproduced, although a faint feature associated with S II is also present at the same wavelength in the spectrum of SN 1991T. As in SN 2005gj, the notch characterizing the spectrum of SN 1991T at 5300 \AA is barely detected in SN 2008J. The imperfect match is not surprising since the spectral decomposition model does not include the coupling between CSI radiation and SN envelope, which should alter the spectral features of the underlying SN. As SN 2008J appears to be as luminous as SN 2005gj (see Fig. 1), we conclude that the emission due to the CSI is also similar. The flux contribution of the underlying SN to the V-band maximum of both SNe is $\sim 60\%$. Similarly to SNe 2002ic and 2005gj, if the CSM is optically thick, the interaction region should not completely cover the SN Ia since its broad features are evident in the spectra. We note that Benetti et al. (2006) argued that SN 2002ic might be better explained by a Type Ic event

¹ H α is missing as it falls between two orders of the echelle spectrum.

like SN 2004aw (Taubenberger et al. 2006), which also shows the presence of Si II, rather than by the CSM-SN Ia scenario suggested by Hamuy et al. (2003). However, in the recent case of PTF11kx, the first spectrum obtained unequivocally shows a 1991T-like SN whose spectrum was only barely affected by CSI (Dilday et al. 2012). The discovery of PTF11kx therefore provides strong support to the interpretation of the other members of the SN 2002ic class as CSM-SNe Ia.

The narrow emission lines and P-Cygni profiles reveal the presence of un-shocked, radially expanding CSM photo-ionized by CSI radiation. The CSM likely originates from winds in the progenitor system, and it is characterized by a velocity $v_w \approx 50 \text{ km s}^{-1}$. This velocity is higher than that of red supergiant (RSG) or asymptotic giant branch (AGB) winds ($\sim 10 \text{ km s}^{-1}$), and much lower than that of Wolf-Rayet (WR) winds (up to 2000 km s^{-1}). Post-AGB stars show wind velocities in the range of $100\text{--}400 \text{ km s}^{-1}$ (Kotak et al. 2004). However, we can not exclude the possibility that the precursor wind was accelerated by photoionization heating as noticed by Aldering et al. (2006) for SN 2005gj. This would make the AGB or RSG wind velocities more compatible with the measured ones. Episodic nova events (like that suggested for PTF11kx) can also give rise to CSM velocities of $50\text{--}100 \text{ km s}^{-1}$ (Dilday et al. 2012). However, PTF11kx shows a complex CSM, with multiple wind velocities which we do not find in SN 2008J.

The broad components that we observe in bright hydrogen lines are probably related to the shock region. The absolute values of the Balmer decrement are higher for the narrow component than for the broad one, indicating that they are produced in different regions. When the CSI dominates the emission, the luminosity of the broad component of $H\alpha$, $L(H\alpha_{\text{broad}})$, is proportional to the kinetic energy dissipated per unit time across the shock front (Salamanca et al. 1998). Therefore, we roughly estimate the mass-loss rate to be $\dot{M} \approx 3 \times 10^{-3} M_{\odot} \text{ yr}^{-1}$. This is slightly lower than the mass-loss rate computed for SN 2002ic (Kotak et al. 2004). Here we have adopted an efficiency factor $\epsilon_{H\alpha} = 0.1$, shock and wind velocities as measured from the full-width-at-zero-intensity (FWZI) of the broad and narrow $H\alpha$ components (6000 and 100 km s^{-1} respectively), and a measured $L(H\alpha_{\text{broad}}) = 1.3 \times 10^{41} \text{ erg s}^{-1}$.

The host galaxy of SN 2008J is a bright spiral galaxy having $M_B = -20.2$ mag (Doyle et al. 2005). Therefore SN 2008J, like PTF11kx and SN 1999E, is not located in an unusual environment as in the case of SNe 1997cy, 2002ic and 2005gj, all of which occurred in faint hosts. The significant amount of MIR-emission found by Fox et al. (2011) at late times (593 days since discovery) indicates the presence of $\sim 0.01 M_{\odot}$ of circumstellar dust. Late time (+380 days) dust emission was also observed in SN 2002ic (Kotak et al. 2004). We conclude that SN 2008J resulted from CSI of a 1991T-like event, similar to SNe 2002ic, 2005gj and PTF11kx. The observations of these objects suggest the idea that more efficient CSI may occur leading to the misidentification of interacting SNe Ia as SNe IIn.

Acknowledgements. We thank J. L. Prieto for sharing spectra of SN 2005gj with us. This research has made use of the Keck Observatory Archive (KOA). This material is based upon work supported by NSF under grants AST-0306969, AST-0607438, and AST-1008343. The Oskar Klein Centre is funded by the Swedish Research Council. J. P. A. and M. H. acknowledge support by CONICYT through FONDECYT grant 3110142, and by the Millennium Center for Supernova Science (P10-064-F). N. B. S. acknowledges support from the Mitchell Institute for Fundamental Physics and Astronomy, NSF grant AST-1008343 and the Mitchell Chair in Observational Astronomy. G. L. is supported by the Swedish Research Council through grant 623-2011-7117. DARK is funded by the DNRF. M. D. S., G. F. and K. M. acknowledge the support by World Premier International Research Center Initiative, MEXT, Japan.

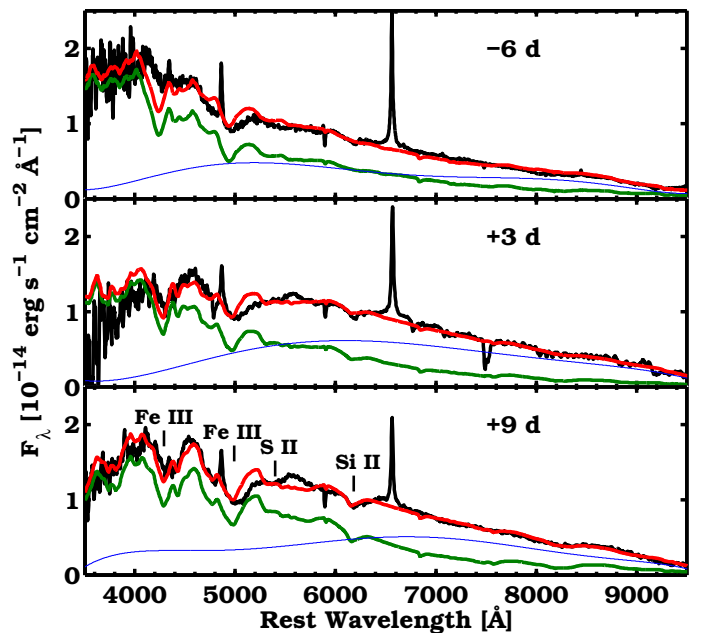


Figure 3: Spectral decomposition of SN 2008J. The de-reddened spectra are well reproduced by the sum (red) of a smooth continuum (blue), powered by the CSI, and of a scaled SN 1991T template spectrum (green). We used SN 1991T templates at the same phase (measured since B_{max}) of the spectra of SN 2008J, which corresponds to 17, 26 and 32 days since explosion.

References

- Aldering, G., Antilogus, P., Bailey, S., et al. 2006, *ApJ*, 650, 510
 Benetti, S., Cappellaro, E., Turatto, M., et al. 2006, *ApJ*, 653, L129
 Cardelli, J. A., Clayton, G. C., & Mathis, J. S. 1989, *ApJ*, 345, 245
 Contreras C., Hamuy, M., Phillips, M. M., et al. 2010, *AJ*, 139, 519
 Chugai, N. N., Chevalier, R. A., & Lundqvist, P. 2004, *MNRAS*, 355, 627
 Deng, J., Kawabata, K. S., Ohyama, Y., et al. 2004, *ApJ*, 605, L37
 Dilday, B., Howell, D. A., Cenko, S. B., et al. 2012, arXiv:1207.1306
 Doyle, M. T., Drinkwater, M. J., Rohde, D. J., et al. 2005, *MNRAS*, 361, 34
 Folatelli, G., Phillips, M. M., Burns, C. R., et al. 2010, *AJ*, 139, 120
 Fox, O. D., Chevalier, R. A., Skrutskie, M. F., et al. 2011, *ApJ*, 741, 7
 Germany, L. M., Reiss, D. J., Sadler, E. M., Schmidt, B. P., & Stubbs, C. W. 2000, *ApJ*, 533, 320
 Hamuy, M., Folatelli, G., Morrell, N., & Phillips, M. M. 2006, *PASP*, 118, 2
 Hamuy, M., Phillips, M. M., Suntzeff, N. B., et al. 2003, *Nature*, 424, 651
 Kotak, R., Meikle, W. P. S., Adamson, A., & Leggett, S. K. 2004, *MNRAS*, 354, L13
 Nugent, P., Kim, A., & Perlmutter, S. 2002, *PASP*, 114, 803
 Poznanski, D., Ganeshalingam, M., Silverman, J. M., & Filippenko, A. V. 2011, *MNRAS*, 415, L81
 Prieto, J. L., Garnavich, P. M., Phillips, M. M., et al. 2007, arXiv:0706.4088
 Rigon, L., Turatto, M., Benetti, S., et al. 2003, *MNRAS*, 340, 191
 Saha, A., Sandage, A., Thim, F., et al. 2001, *ApJ*, 551, 973
 Salamanca, I., Cid-Fernandes, R., Tenorio-Tagle, G., et al. 1998, *MNRAS*, 300, L17
 Schlafly, E. F., & Finkbeiner, D. P. 2011, *ApJ*, 737, 103
 Sternberg, A., Gal-Yam, A., Simon, J. D., et al. 2011, *Science*, 333, 856
 Stritzinger, M., Folatelli, G., & Morrell, N. 2008, *CBET*, 1218, 1
 Taubenberger, S., Pastorello, A., Mazzali, P. A., et al. 2006, *MNRAS*, 371, 1459
 Theureau, G., Bottinelli, L., Coudreau-Durand, N., et al. 1998, *A&AS*, 130, 333
 Thrasher, P., Li, W., & Filippenko, A. V. 2008, *CBET*, 1211, 1
 Turatto, M., Benetti, S., & Cappellaro, E. 2003, *From Twilight to Highlight: The Physics of Supernovae*, ed. W. Hillebrandt & B. Leibundgut (Berlin: Springer), 200
 Turatto, M., Suzuki, T., Mazzali, P. A., et al. 2000, *ApJ*, 534, L57
 Wang, X., Li, W., Filippenko, A. V., et al. 2008, *ApJ*, 675, 626
 Wood-Vasey, W. M., Wang, L., & Aldering, G. 2004, *ApJ*, 616, 339

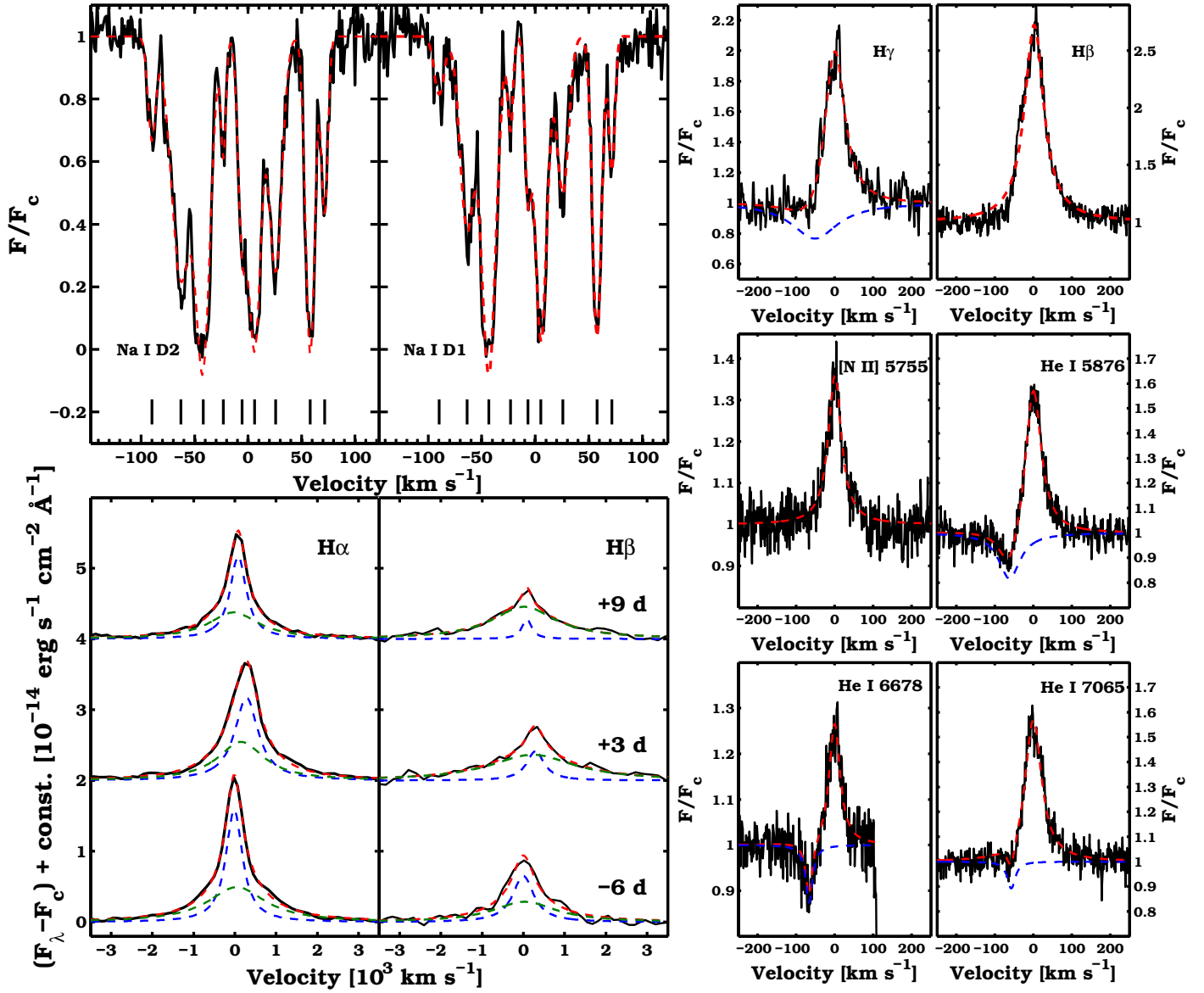


Figure 4: (*Top-left panels*) Na I D absorption features in the high resolution spectrum of SN 2008J. Several components are present and their peak positions are indicated by black solid lines. The features are fit with the sum of 9 Gaussian functions, the best fit is shown in red. Velocity is plotted in the SN rest frame, as determined from the narrow emission line peaks in the same high resolution spectrum (*Bottom-left panels*) H α and H β sequences from the low resolution spectra, shown after low-order polynomial continuum subtraction. Each profile is well fit by the sum (in red) of two Lorentzian components (in blue and green). (*Right panels*) Narrow emission lines in the high-resolution spectrum of SN 2008J. Each line has been fit with a Lorentzian profile for the emission and one for the absorption when detected. The absorption component is shown in blue, the total best fit in red. The spectrum is presented in velocity scale, where the zero velocity corresponds to the emission peak position.

Table 1. Optical and near-infrared photometry of the local sequences in the standard system

STAR	α (2000)	δ (2000)	u' (mag)	g' (mag)	r' (mag)	i' (mag)	B (mag)	V (mag)	Y (mag)	J (mag)	H (mag)	K_s (mag)
01	02:34:42.34	-10:50:57.55	11.387(020)	11.180(014)
02	02:34:32.13	-10:54:08.89	17.014(032)	15.323(008)	14.743(007)	14.517(008)	15.767(014)	14.979(008)	13.778(020)	13.540(020)
03	02:34:21.64	-10:53:03.59	17.948(024)	15.706(010)	14.904(007)	14.629(008)	16.230(020)	15.263(008)	13.860(017)	13.544(014)
04	02:34:29.09	-10:54:11.99	18.864(113)	16.284(010)	14.999(011)	14.373(012)	16.974(017)	15.591(010)	13.295(020)	12.910(020)
05	02:34:20.76	-10:54:10.12	17.203(033)	16.091(008)	15.681(007)	15.523(008)	16.427(016)	15.842(008)	14.885(020)	14.667(020)
06	02:34:12.06	-10:48:14.11	17.813(016)	16.282(007)	15.713(007)	15.506(008)	16.719(016)	15.952(008)
07	02:34:21.89	-10:49:23.30	19.563(077)	17.130(010)	16.179(007)	15.827(009)	17.686(017)	16.623(008)	14.995(026)	14.559(072)	13.934(053)	13.884(014)
08	02:34:22.98	-10:52:35.72	18.622(054)	17.143(012)	16.583(007)	16.364(008)	17.572(012)	16.817(008)	15.677(017)	15.415(014)
09	02:34:22.67	-10:52:19.16	20.497(135)	17.842(020)	16.526(007)	15.899(008)	18.555(011)	17.141(008)	14.886(014)	14.472(014)
10	02:34:33.03	-10:51:38.70	18.456(035)	17.529(009)	17.180(007)	17.051(008)	17.814(016)	17.317(008)	16.456(069)	16.270(020)
11	02:34:37.60	-10:51:12.64	20.776(166)	18.090(017)	16.888(008)	16.330(008)	18.748(015)	17.455(009)	15.361(028)	14.941(014)
12	02:34:38.22	-10:52:13.37	18.861(024)	17.959(009)	17.576(007)	17.422(008)	18.300(018)	17.728(008)	16.880(024)	16.664(020)
13	02:34:09.23	-10:52:55.63	20.654(160)	18.193(010)	17.122(007)	16.702(008)	18.802(023)	17.624(008)
14	02:34:13.94	-10:49:16.61	19.598(076)	19.070(034)	18.926(027)	18.916(034)	19.306(064)	19.001(038)	...	18.004(085)
15	02:34:21.44	-10:47:44.38	...	19.517(021)	18.174(008)	17.245(015)	20.342(043)	18.755(020)	16.029(020)	15.635(020)
16	02:34:32.12	-10:48:58.86	...	19.837(020)	18.435(026)	16.847(023)	20.711(060)	19.052(020)	15.148(031)	14.655(014)
17	02:34:16.79	-10:48:28.44	16.721(017)	16.251(014)
18	02:34:29.84	-10:52:05.95	17.243(056)	16.815(024)
19	02:34:22.32	-10:52:44.90	17.169(035)	16.920(052)
20	02:34:20.29	-10:51:52.74	17.283(029)	16.895(099)
21	02:34:23.43	-10:49:01.24	17.813(081)	17.448(090)	16.873(145)	...
22	02:34:20.91	-10:52:20.60	17.917(063)	17.486(063)
23	02:34:29.18	-10:51:05.65	18.096(037)	17.647(106)	16.812(276)	16.825(298)
24	02:34:36.21	-10:51:16.02	18.238(094)	17.974(099)
25	02:34:15.59	-10:49:28.42	18.354(138)	18.428(100)
26	02:34:19.40	-10:49:06.60	18.397(085)	18.097(120)	17.518(273)	...
27	02:34:32.14	-10:51:48.89	16.058(080)	15.608(028)
28	02:34:34.53	-10:48:45.14	18.190(081)
29	02:34:17.50	-10:49:57.54	17.694(052)	17.245(079)
30	02:34:16.18	-10:49:55.88	18.114(256)	17.686(049)
31	02:34:19.77	-10:47:04.88	17.806(049)	17.604(071)
32	02:34:23.86	-10:46:19.13	18.206(070)	18.340(128)

Note. — Uncertainties given in parentheses in thousandths of a magnitude correspond to an rms of the magnitudes obtained on photometric nights.

Table 2. Optical photometry of SN 2008J in the natural system.

JD - 2, 453, 000	Phase ^a	<i>u</i> (mag)	<i>g</i> (mag)	<i>r</i> (mag)	<i>i</i> (mag)	<i>B</i> (mag)	<i>V</i> (mag)
1480.69	-7.66	15.4 ^b
1481.70	-6.65	15.4 ^b
1484.54	-3.81	...	16.633(009)	15.392(005)	14.994(004)	17.231(012)	16.018(008)
1486.59	-1.76	18.609(057)	16.616(008)	15.333(006)	14.936(006)	17.225(011)	15.972(008)
1488.56	+0.21	18.624(051)	16.582(006)	15.306(005)	14.885(005)	17.231(013)	15.934(007)
1490.55	+2.20	18.824(029)	16.579(007)	15.249(005)	14.835(006)	17.224(009)	15.917(007)
1492.58	+4.23	18.897(042)	16.568(007)	15.210(006)	14.778(008)	17.234(010)	15.885(008)
1493.59	+5.24	18.845(030)	16.573(006)	15.215(007)	14.780(006)	17.235(009)	15.876(007)
1494.54	+6.19	18.918(030)	16.593(009)	15.207(006)	14.780(008)	17.263(009)	15.878(007)
1497.54	+9.19	19.044(049)	16.595(007)	15.173(004)	14.746(005)	17.271(009)	15.849(008)
1499.55	+11.20	...	16.611(006)	15.177(004)	14.751(006)	17.325(009)	15.851(006)
1515.52	+27.17	19.578(124)	17.018(018)	15.395(005)	14.857(005)	17.821(017)	16.157(008)

Note. — Values in parentheses are 1σ measurement uncertainties in millimag. Imaging was performed with a Site3 detector attached to the Swope.

^aDays since B_{max} (JD 2454488.35).

^bUnfiltered magnitudes from discovery and confirmation images (Thrasher et al. 2008).

Table 3. NIR photometry of SN 2008J in the natural system.

JD - 2, 453, 000	Phase ^a	<i>Y</i> (mag)	<i>J</i> (mag)	<i>H</i> (mag)	<i>K_s</i> (mag)
1485.60	-2.75	14.090(011)	13.877(018)	13.442(024)	...
1491.55	+3.20	13.934(011)	13.734(020)	13.268(023)	...
1494.59	+6.24	13.844(022)	13.688(023)	13.277(034)	13.140(018)
1496.55	+8.20	13.775(031)	13.641(044)	13.286(034)	13.136(011)
1498.58	+10.23	13.840(011)	13.561(011)
1511.53	+23.18	13.905(043)	13.670(013)
1806.65	+318.30	16.776(024)

Note. — Values in parentheses are 1σ measurement uncertainties in millimag. The imaging was performed with RetroCam attached to the Swope.

^aDays since B_{max} (JD 2454488.35).

Table 4. Spectroscopic observations of SN 2008J.

Date (UT)	Julian Date JD - 2, 453, 000	Phase ^a (days)	Telescope	Instrument	Range (Å)	Resolution (FWHM Å)	Integration (sec)
2008 Jan. 17	1482.57	-5.78	NTT	EMMI	3200 – 10200	6-9	3 × 300
2008 Jan. 18	1483.59	-4.76	NTT	SOFI	9400 – 25000	20-30	1 × 2100
2008 Jan. 23	1488.72	+0.37	Keck I	HIRES	4110 – 8360	0.12	2 × 900
2008 Jan. 26	1491.57	+3.22	Du Pont	B&C	3518 – 9715	8	1 × 400
2008 Feb. 01	1497.55	+9.20	Du Pont	B&C	3510 – 9713	8	3 × 500

^aDays since B_{max} (JD 2454488.35).

Table 5. Parameters from the narrow emission line fit.

Line	λ_c (Å)	FWHM (km s ⁻¹)
H γ λ 4341	4340.9	62 ± 4
H β λ 4861	4861.8	77 ± 4
[N II] λ 5755	5755.0	44 ± 2
He I λ 5876	5876.2	51 ± 2
He I λ 6678	6678.7	33 ± 2
He I λ 7065	7065.8	49 ± 1

Table 6. Peak magnitudes of SN 2008J.

Filter	Phase ^a (days)	Peak (apparent mag)	Peak (absolute mag)	Peak (absolute mag)
			$R_V = 1.5$ $E(B - V)_{\text{tot}} = 1.3^{+0.3}_{-0.2}$	$R_V = 3.1$ $E(B - V)_{\text{tot}} = 0.8^{+0.2}_{-0.1}$
<i>u</i>	< -1.8	< 18.59	< -19.72 ^{+1.01} _{-0.69}	< -19.34 ^{+1.00} _{-0.52}
<i>B</i>	0	17.22±0.01	-20.25 ^{+0.82} _{-0.56}	-20.24 ^{+0.88} _{-0.46}
<i>g</i>	+4.4	16.57±0.01	-20.38 ^{+0.70} _{-0.48}	-20.58 ^{+0.80} _{-0.42}
<i>V</i>	+10.6	15.85±0.01	-20.31 ^{+0.52} _{-0.36}	-20.81 ^{+0.68} _{-0.36}
<i>r</i>	+11.5	15.17±0.01	-20.52 ^{+0.41} _{-0.28}	-21.12 ^{+0.59} _{-0.31}
<i>i</i>	+11.7	14.75±0.01	-20.34 ^{+0.26} _{-0.19}	-21.04 ^{+0.45} _{-0.25}
<i>Y</i>	+13.3	13.79±0.01	-20.73 ^{+0.14} _{-0.10}	-21.24 ^{+0.28} _{-0.16}
<i>J</i>	+14.6	13.59±0.02	-20.83 ^{+0.11} _{-0.09}	-21.23 ^{+0.22} _{-0.13}
<i>H</i>	> +8.2	< 13.27	< -21.04 ^{+0.09} _{-0.07}	< -21.30 ^{+0.16} _{-0.10}
<i>K_s</i>	> +8.2	< 13.14	< -21.09 ^{+0.07} _{-0.06}	< -21.26 ^{+0.11} _{-0.08}

Note. — Uncertainties in the phase are ~0.1 days for the optical passbands, ~1 day for the NIR. Errors in the absolute magnitude are given by the uncertainties in the extinction and in the distance modulus (0.04 mag).

^aDays since B_{max} (JD 2454488.35).